Katholieke Universiteit Leuven

Departement Elektrotechniek

ESAT-SISTA/TR 1999-80

Hybrid Subband/Frequency–Domain Adaptive Systems [1]

Koen Eneman, Marc Moonen [2]

Published in Signal Processing vol. 81(1), pp. 117-136
January 2001

[1]This report is available by anonymous ftp from *ftp.esat.kuleuven.ac.be* in the directory *pub/SISTA/eneman/reports/99-80.ps.gz*

[2]ESAT (SISTA) - Katholieke Universiteit Leuven, Kardinaal Mercierlaan 94, 3001 Leuven (Heverlee), Belgium, Tel. 32/16/321809, Fax 32/16/321970, WWW: *http://www.esat.kuleuven.ac.be/sista*. E-mail: *koen.eneman@esat.kuleuven.ac.be*. The authors would like to thank Ian Proudler for his contribution to the presented work. Marc Moonen is a Research Associate with the F.W.O. (Fund for Scientific Research – Flanders). This research work was carried out at the ESAT laboratory of the Katholieke Universiteit Leuven, in the frame of the Belgian State Interuniversity Poles of Attraction Programme – IUAP P4–02 (1997–2001) : Modeling, Identification, Simulation and Control of Complex Systems, Concerted Research Action MIPS ('Model–based Information Processing Systems') and GOA–MEFISTO–666 of the Flemish Government, Research Project F.W.O. nr. G.0295.97 ('Design and implementation of adaptive digital signal processing algorithms for broadband applications') and IWT project AUT/970517: MUSETTE ('Multimicrophone Signal Enhancement Techniques for handsfree telephony and voice controlled systems'). The scientific responsibility is assumed by its authors.

Hybrid Subband/Frequency–Domain Adaptive Systems

Koen Eneman Marc Moonen
ESAT – Katholieke Universiteit Leuven
Kardinaal Mercierlaan 94, B–3001 Heverlee – Belgium
phone : +32/16321809 +32/16321060
fax : +32/16321970
email : koen.eneman@esat.kuleuven.ac.be
marc.moonen@esat.kuleuven.ac.be

Abstract

For many years now, subband and frequency–domain adaptive filtering techniques have been proposed for the identification of high–order FIR systems. Classical LMS–based algorithms are less attractive as their computational load is higher and their convergence behaviour for coloured inputs is worse.
Subband processing has many desirable properties. However, when used to implement adaptive filters, various effects (such as residual errors and slow convergence due to aliasing) occur and reduce performance.
On the other hand, it is known that frequency–domain adaptive filters do not suffer from these problems despite being (nearly) equivalent to subband adaptive filters, be it with "poor" filter banks (modulated sinc frequency responses).
In this paper the operation of the frequency–domain techniques are unravelled and explained in the "subband jargon" and among other things it will be shown how aliasing is compensated for in the frequency–domain approach. This paper aims at generalising frequency–domain aliasing–compensation techniques to subband adaptive systems.
Further, some design criteria for subband adaptive systems are formulated. Three realisation conditions and an alternative adaptation scheme will be proposed. Standard subband adaptive filters cannot fulfil all conditions, whereas for frequency–domain based algorithms the design criteria are met.

1 Introduction

Multirate adaptive schemes have been a topic of interest for many years now [1][10]. They are employed to identify high–order FIR systems and are a promising alternative for the classical LMS algorithm. For this kind of application the

LMS algorithm is less attractive as it has a higher complexity and its convergence behaviour is often worse. Still, with the available multirate techniques, it is difficult to meet all the requirements.
Frequency–domain techniques are well understood. They are based on a translation of the Block–(N)LMS algorithm to the frequency domain, and hence their performance is very tractable. On the other hand, *subband adaptive filters* —at first sight— may have a lower complexity (whenever critical downsampling is used, instead of for instance 2–fold oversampling which is typical for frequency–domain adaptive filters) and better performance (owing to the fact that after appropriate subsampling each subband signal will have a flatter spectrum than the fullband signal). Unfortunately, this picture of the subband approach is certainly too optimistic.
Subband adaptive filters and frequency–domain based techniques are typically considered as being different approaches. In this paper we will consider the frequency–domain algorithm as a special case of subband adaptive filtering and point out why frequency–domain techniques are better from certain perspectives. The ultimate goal is then to transplant their desirable properties to the subband approach.

2 Subband Adaptive Filtering

2.1 General setup

The general setup for a subband adaptive system is shown in **Figure 1**. The loudspeaker and microphone are added for convenience, indicating how the adaptive filter structure may be employed in an acoustic echo cancellation setup. While acoustic echo cancellation has been a driving application for many researchers in this field, all results obviously apply to other applications too.
The input signals x and d are fed into identical M–band analysis filter banks. After subsampling with a factor L, (mostly LMS–based) adaptive filtering is done in each subband. The outputs of the subband adaptive filters are recombined in the synthesis filter bank leading to the final output. The ideal characteristics of the analysis bank filters H_i and synthesis bank filters G_i are shown (ideal bandpass filters). Due to aliasing effects, this setup will only work for $M \geqslant L$.
By splitting signals into subbands and subsequent subsampling faster (initial) convergence and better tracking properties are hoped for. A second advantage of subband systems over classical fullband adaptation is the lower achievable implementation cost (due to downsampling).

2.2 Polyphase implementation

The analysis bank filters are immediately followed by downsamplers. Hence it is cheaper to do all filter operations at the downsampled rate. Figure 1 can be re–arranged resulting in **Figure 2**. $\mathbf{H}(z)$ and $\mathbf{G}(z)$ are respectively called the

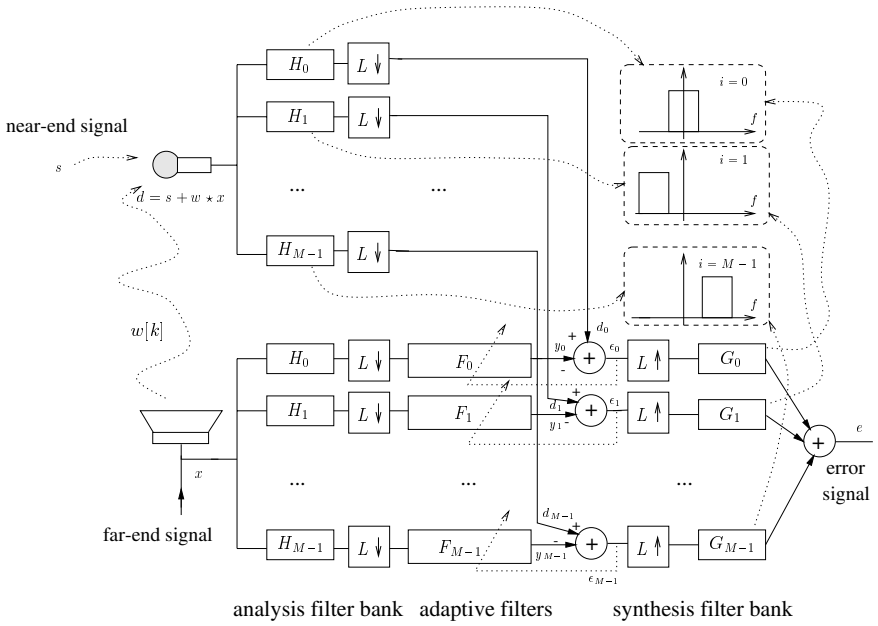


Figure 1: Subband adaptive filter with ideal filter banks : echo cancellation setup

analysis and synthesis polyphase matrix. Element (i, j) of $\mathbf{H}(z)$ is

$$[\mathbf{H}(z)]_{ij} = H_{i_{j:L}}(z) \qquad \begin{cases} i = 0 \to M-1 \\ j = 0 \to L-1 \end{cases} \tag{1}$$

$H_{i_{j:L}}(z)$ is the j–th out of L polyphase components of the i–th subband filter $h_i[k]$, in other words the z–transform of $h_i[j + Lk]$. Similarly,

$$[\mathbf{G}(z)]_{ij} = G_{i_{j:L}}(z) \qquad \begin{cases} i = 0 \to M-1 \\ j = 0 \to L-1 \end{cases} \tag{2}$$

2.3 DFT modulated subband adaptive filters

Subband adaptive systems are often based on DFT modulated filter banks. A DFT modulated filter bank consists of M subband filters which are derived from a single prototype filter $h_0[k]$:

$$h_i[k] = h_0[k] e^{-j\frac{2\pi ki}{M}} \qquad i = 0 \to M-1 \tag{3}$$

$$\Leftrightarrow$$

$$H_i(z) = H_0(e^{j\frac{2\pi i}{M}} z) \tag{4}$$

The analysis filters are frequency shifted versions of each other and the complete set of M filters covers the whole frequency spectrum.

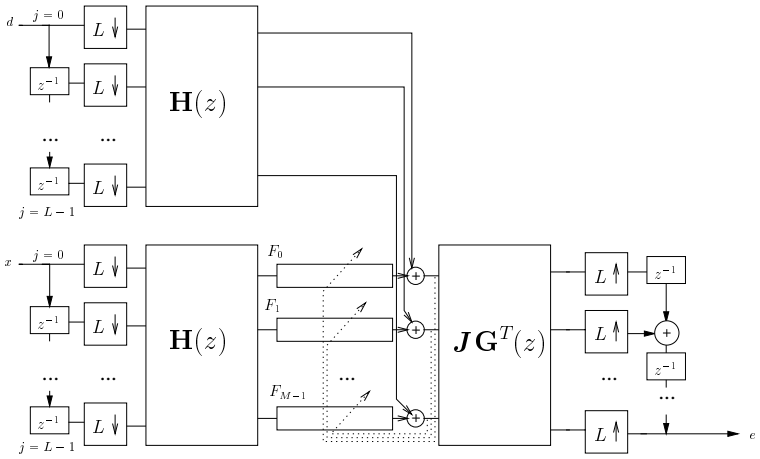


Figure 2: Subband adaptive filter : polyphase implementation

Cosine or DCT modulated filter banks are a well–known alternative for DFT modulated filter banks [12]. They are often based on the QMF–principle and are used in audio coding for instance. Cosine modulated filters are real and hence have a positive and negative frequency band. The positive and negative frequent subbands tend to overlap when the subband signals are downsampled and as a consequence aliasing is inserted in the subbands. This is detrimental for the convergence of the subband adaptive filters (see also section 2.4). DFT modulated filter banks are therefore more appropriate for subband adaptive filtering applications.
DFT modulated filter banks may be implemented efficiently using polyphase decomposition and fast signal transforms. In [2] a general framework for DFT modulated subband systems was proposed. A DFT modulated filter bank with L–fold downsampling can be implemented as a tapped delay line of size L followed by a structured $M \times L$ matrix $\mathbf{B}(z)$, containing polyphase components of the prototype h_0, and an $M \times M$ DFT matrix $\mathbf{F}$. For DFT modulated filter banks figure 2 can be redrawn resulting in **Figure 3**.
It can be shown that element (i, j) of $\mathbf{B}(z)$ is given by :

$$\begin{array}{rcll} B_{ij}(z) & = & z^{-l} E_{(j+lL):K}(z^J) & \text{if } (i-j) \bmod g = 0 \\ & = & 0 & \text{if } (i-j) \bmod g \neq 0 \end{array} \tag{5}$$

$$i, j \geqslant 0,\ (j + lL) \bmod M = i,\ J = \frac{M}{g},\ g = \gcd(M, L),\ K = \frac{ML}{g}$$

$E_{k:K}(z)$ is the k–th out of K polyphase components of the prototype filter h_0. The synthesis bank is constructed in a similar fashion with an $L \times M$ matrix $\mathbf{C}(z)$.

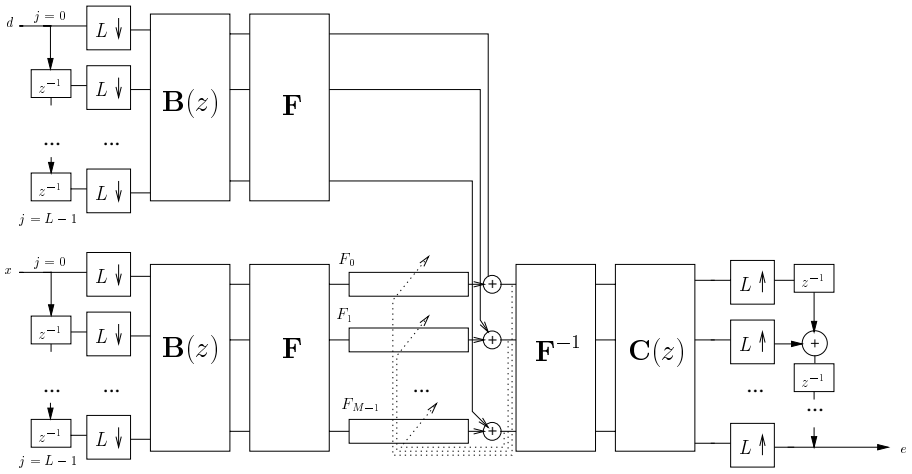


Figure 3: DFT modulated subband adaptive filter

2.4 Downsampling and aliasing

Critically downsampled subband schemes

For critically downsampled subband systems $M = L$. Critically downsampled subband systems seem attractive because optimal computational savings can be obtained as L is as high as possible.
In the (apparently) ideal case with *infinite order* analysis and synthesis filters the prototype filters are ideal lowpass and their impulse response is a sinc function. A causal implementation however introduces an infinite delay which obviously is intolerable. *Finite order filters*, however, have a non–negligible transition band and therefore critically downsampled subband systems will always insert some *aliasing* in the subbands. Aliasing is detrimental for the overall convergence of the adaptive filters. In [8] it is shown that critically downsampled subband adaptive systems suffer from a residual error which is considerable unless cross filters are included between neighbouring subbands. Cross filters again increase the complexity, which is unwanted. Furthermore, cross filters fail to converge quickly to the optimal solution. This suggests the use of oversampled subband schemes for which $M > L$.

2–fold oversampled subband systems

In this case the subband signals are subsampled 2 times less compared to the critical scheme, i.e. $M = 2L$. From a computational point of view 2–fold oversampled subband systems seem to be less interesting as —roughly speaking— their implementation cost is 4 times higher compared to the case with critical subsampling : the required subband adaptive filters are roughly twice as long and operate at twice the sampling rate. As will be shown later on, frequency–domain adaptive filters can be cast in the subband approach as a

special kind of oversampled subband system. For a typical parameter setting for the frequency–domain adaptive filter the oversampling factor $\frac{M}{L}$ is equal to 2. Frequency–domain adaptive filters have desirable convergence properties, and hence provide probably the best solution in those cases where 2–fold oversampling is affordable.

In conclusion, the above examples represent 2 extremes : the critically downsampled scheme, interesting at first sight from a computational point of view but with poor performance, and the 2–fold oversampled system with the frequency–domain scheme in mind, more expensive but with desirable convergence properties. The ultimate goal may then be to find acceptable performance with $\frac{M}{2} \leqslant L \leqslant M$.

3 Realisation Conditions for Subband Adaptive Systems

In this paragraph some design criteria for subband adaptive systems are formulated, which should lead to subband adaptive filters exhibiting better properties, similar to what can be obtained with frequency–domain techniques (see section 4). Frequency–domain adaptive algorithms typically use simple filter banks and often have an oversampling factor equal to 2. Most subband adaptive systems perform better on this part as their oversampling factors are normally less than 2 and more advanced filter banks are employed. Bringing together both ideas into a "hybrid" approach should ultimately lead to a better overall performance. An analysis/synthesis filter bank set is therefore (preferably) designed such that 3 realisation conditions are met [4] :

3.1 Frequency selectivity

The *analysis filters* should be frequency selective. This reduces the amount of aliasing components inserted in the subbands. Inter–subband aliasing has an inhibitive effect on the convergence of the adaptive filters (cf. paragraph 2.4). At first sight, the frequency characteristics of the *synthesis bank* do not seem to have an influence on the convergence of the subband adaptive filters (see figure 1 or 3). In paragraph 5 however, we will introduce an alternative adaptation scheme for which the adaptation of the subband filter coefficients depends on the synthesis filter bank. In that case the characteristics of the synthesis bank may be important.
Highly frequency selective filter banks introduce a substantial processing delay. This puts a constraint on the frequency selectivity, and hence on the downsampling factor L as delay constraints make subband schemes unattractive. On the other hand, computational savings are more or less proportional to L.

3.2 Perfect reconstruction

Both the far–end signal x and near–end signal d ($d = s + w \star x$) are passed through the filter bank system (see figure 1). Ideally, the far–end signal is completely suppressed by the adaptive filtering operations and the desired part s of near–end signal is passed to the output of the subband scheme without distortion, being an exact (delayed) copy of the near–end input. Perfect reconstruction is obtained when (see figure 2)

$$\boldsymbol{J}\mathbf{G}^T(z)\mathbf{H}(z) = z^{-\delta}\mathbf{I}_L. \tag{6}$$

The smallest δ is determined such that Eq. 6 is fulfilled and such that both the analysis and synthesis filters are causal and hence implementable.
In the case of DFT modulated filter banks the perfect reconstruction property reduces to (see figure 3)

$$\mathbf{C}(z)\mathbf{B}(z) = z^{-\delta}\mathbf{I}_L. \tag{7}$$

Condition 7 can be relaxed to $\mathbf{C}(z)\mathbf{B}(z) \approx z^{-\delta}\mathbf{I}_L$ leading to nearly perfect reconstruction up to a delay.
In order to fulfil Eq. 7, $\mathbf{C}(z)$ has to be a left inverse of $\mathbf{B}(z)$. This left inverse exists if $M \geqslant L$. However, the synthesis filter bank which is obtained by inversion is not necessarily FIR or DFT modulated. In the most general case $\mathbf{C}(z)$ is a dense rational matrix and hence, the corresponding filter bank is IIR.
Assume that the Smith–McMillan decomposition of the polynomial matrix $\mathbf{B}(z)$ is given by (see [12])

$$\mathbf{B}(z) = \mathbf{R}(z)\mathbf{D}(z)\mathbf{T}(z). \tag{8}$$

$\mathbf{R}(z)$ and $\mathbf{T}(z)$ are respectively $M \times M$ and $L \times L$ unimodular matrices. This implies that their determinant is a non–zero constant or equivalently, that they can be decomposed as a product of elementary matrices [12]. $\mathbf{D}(z)$ is an $M \times L$ pseudo–diagonal matrix which can be expressed as

$$\mathbf{D}(z) = \begin{bmatrix} \mathbf{D}_1(z) \\ \mathbf{0}_{(M-L)\times L} \end{bmatrix} = \begin{bmatrix} d_1(z) & & \\ & \ddots & \\ & & d_L(z) \\ & \mathbf{0}_{(M-L)\times L} & \end{bmatrix}. \tag{9}$$

The synthesis bank $\mathbf{C}(z)$ which can be combined with $\mathbf{B}(z)$ to ensure perfect reconstruction, is

$$\begin{aligned} \mathbf{C}(z) &= \mathbf{B}^{\dagger}(z) + \mathbf{N}(z) && (10) \\ &= \mathbf{T}^{-1}(z)\left(\begin{bmatrix}\mathbf{D}_1^{-1}(z) & \mathbf{0}_{L\times(M-L)}\end{bmatrix} + \begin{bmatrix}\mathbf{0}_{L\times L} & \mathbf{X}(z)\end{bmatrix}\right)\mathbf{R}^{-1}(z). && (11) \end{aligned}$$

$\mathbf{N}(z)$ is an $L \times M$ matrix which lies in the left null space of $\mathbf{B}(z)$. $\mathbf{X}(z)$ is an $L \times (M-L)$ random rational matrix. $\mathbf{R}(z)$ and $\mathbf{T}(z)$ are unimodular polynomial matrices, so their determinant is a non–zero constant, independent of z. Hence, their inverse $\mathbf{R}^{-1}(z) = \mathrm{adj}\mathbf{R}(z)/\mathrm{det}\mathbf{R}(z)$ is also polynomial.
In the most general case $\mathbf{D}_1^{-1}(z)$ is rational and the synthesis filter bank is IIR.

A true FIR inverse can be obtained if $\mathbf{D}_1(z)$ has monomial diagonal elements and $\mathbf{N}(z)$ is polynomial.
In order to obtain a DFT modulated synthesis bank $\mathbf{C}(z)$ should be a polynomial matrix, with a structure analogue to that of $\mathbf{B}(z)$ (see Eq. 5). In this case the synthesis filters have equal spectral characteristics, up to a frequency shift. Furthermore, a cheap implementation would be possible thanks to the special, sparse structure of $\mathbf{C}(z)$ (Eq. 5). It appears that the inverse row and column operations $\mathbf{T}^{-1}(z)$ and $\mathbf{R}^{-1}(z)$ which act on $\left[\mathbf{D}_1^{-1}(z) \quad \mathbf{0}\right]$ put $\mathbf{B}^\dagger(z)$ in the desired format i.e. a structure analogue to that of $\mathbf{B}(z)$. If $\mathbf{N}(z)$, based on a random $\mathbf{X}(z)$, is added to $\mathbf{B}^\dagger(z)$ the structure will not be maintained in general. If now $\mathbf{B}(z)$ is designed to be para–unitary, i.e.

$$\tilde{\mathbf{B}}(z)\mathbf{B}(z) = \mathbf{I}_L, \tag{12}$$

in which $\tilde{\mathbf{B}}(z) = \mathbf{B}_*^T(z^{-1})$ (see [12]), $\mathbf{C}(z)$ can be chosen to be the paraconjugate of $\mathbf{B}(z)$:

$$\mathbf{C}(z) = \tilde{\mathbf{B}}(z), \tag{13}$$

i.e. $\mathbf{C}(z)$ is obtained by transposing $\mathbf{B}(z)$, replacing all filter coefficients by their complex conjugate and replacing z by z^{-1}. In this case the synthesis filters have the same frequency characteristics as the analysis filters and again perfect reconstruction is ensured. Perfect reconstruction design for critically downsampled DFT modulated filter banks is well–known [12] and relies on this para–unitariness property, but as discussed in sections 2.3 and 2.4 these maximally decimated filter banks are not appropriate for subband adaptive filtering applications. Some references on perfect reconstruction design for oversampled DFT modulated filter banks can be found in more recent publications such as [2] and [5].
Finally, note that adaptive filtering operations need to be done in each subband. Perfect reconstruction will only hold for the desired part of the near–end signal (upper branch of figure 1), as the adaptive filters in between the analysis and synthesis filter bank (lower branch of figure 1) do not preserve perfect reconstruction.

3.3 Perfect path modelling

Splitting signals into subbands seems very promising since for coloured inputs, fullband convergence may be slow due to ill–conditioned covariance matrices. In the subband case, each subband signal will have a flatter spectrum after appropriate subsampling, leading to improved convergence. Instead of a single fullband L_{FB}–taps FIR filter, M subband filters of, say, $L_{SB} = \frac{L_{FB}}{L}$ taps are used. As the adaptive computations as well as the filter bank convolutions can be done at a reduced sampling rate, the subband approach is supposed to give a better performance at a lower cost.
It is clear that this picture is certainly too optimistic. Whereas critically downsampled subband schemes inherently suffer from subband aliasing, in oversampled subband adaptive systems reduced aliasing distortion is traded off for extra computational costs and slower steady–state convergence. Moreover, the

assumption of having M subband filters with reduced length $\frac{L_{FB}}{L}$ seems to be quite wrong.
One can prove [7] that in the case of an M–band, L–fold downsampled ideally frequency selective DFT modulated filter bank the i–th subband adaptive filter should converge to $\hat{w}_i[k]$:

$$\hat{w}_i[k] = \left(w[m] \star \left(e^{-j\frac{2\pi im}{M}} \mathrm{sinc}(\frac{\pi m}{L}) \right) \right)_{L\downarrow}, \tag{14}$$

i.e., $\hat{w}_i[k]$ can be obtained by downsampling the convolution of the impulse response of the unknown system $w[k]$ and a modulated double–sided sinc. Even when $w[k]$ represents an FIR filter, the $\hat{w}_i[k]$ in general are not FIR. The adaptive identification process therefore has to track (many) more than $\frac{L_{FB}}{L}$ samples and due to the spreading out in both directions of the time axis, an extra delay has to be inserted in the upper signal path (see **Figure 4** for an experimental verification). Neglecting the extra delay and the additional subband filter taps

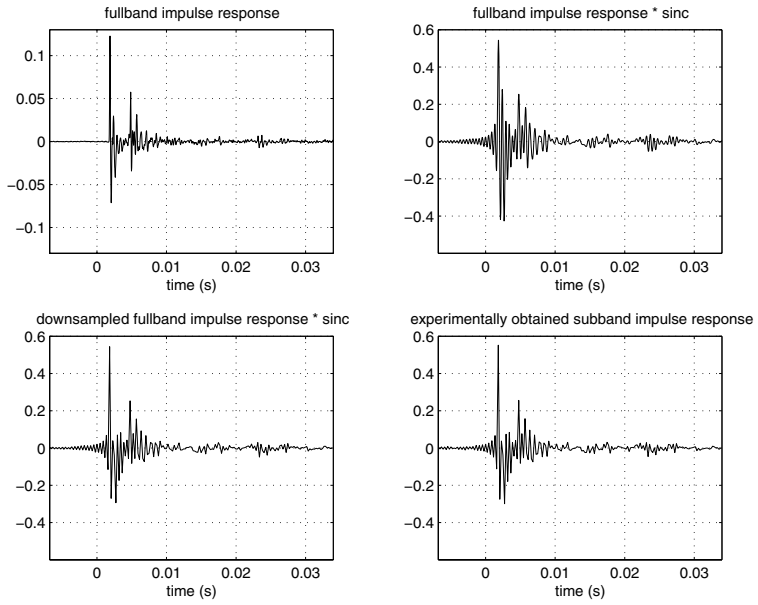


Figure 4: The first (left, top) subplot shows a real acoustic impulse response obtained from measured data. In subplot 2 (right, top), the acoustic impulse response is convolved with $\mathrm{sinc}(\frac{\pi k}{10})$. In subplot 3 (left, bottom), the downsampled version of subplot 2 is shown, corresponding to Eq. 14 ($L = 10, i = 0$). Then, the data were filtered with a sharp lowpass filter with cutoff 0.05 and were 10–fold downsampled. The impulse response between the subband data was identified and is shown in subplot 4. Apart from some measurement noise it matches the downsampled convolution which was theoretically obtained following Eq. 14 (subplot 3).

strongly limits the convergence of the adaptive filters and leads to a residual

undermodelling error. This is illustrated by means of the following experiment. A randomly generated FIR system of order 15 was identified using a white noise input. 3 different adaptive algorithms are compared :

a) a 6–band, 4–fold downsampled standard subband adaptive system (see figure 1) was designed with subband adaptive filters having length $\frac{L_{FB}}{L} = 4$. The NLMS–algorithm was used to adapt the subband filters. Both the analysis and the synthesis filters are FIR, DFT modulated and are of order 51. The filterbank set was designed to guarantee perfect reconstruction (Eq. 7). The frequency characteristic of the analysis prototype filter is shown in **Figure 5**. From **Figure 6** it is clear that for the standard

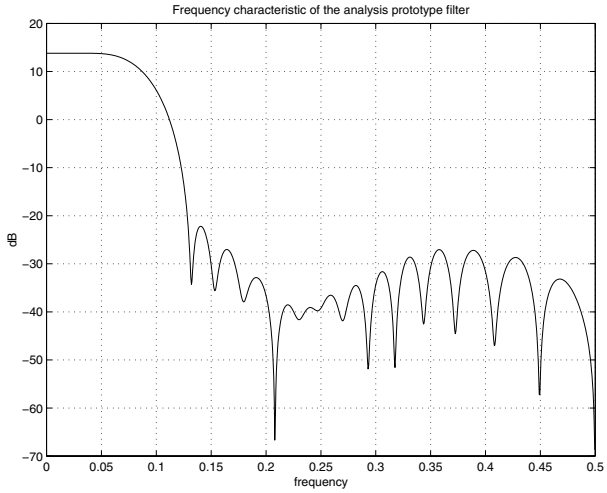


Figure 5: Frequency characteristic of the analysis prototype filter

subband adaptive filter a considerable undermodelling error remains.

b) The same subband system was then used, adding extra filter and anti–causal taps to allow a better modelling. The subband filters then had 2 anti–causal taps and a total of 10 filter taps each. The steady–state undermodelling error is strongly reduced.

c) Finally, the error convergence curve of a well–known frequency–domain adaptive filter, the so–called normalised constrained PBFDAF (Eq. 20–24) is also shown on figure 6. It will be proven in paragraph 4.3 that the PBFDAF can be considered as a kind of subband adaptive system. The subband adaptive filters of the PBFDAF used in this experiment were of length 4, and hence, having the same number of parameters, the PBFDAF clearly outperforms the standard subband adaptive scheme. Apparently, perfect modelling is possible with the PBFDAF as the residual error curve goes to 0.

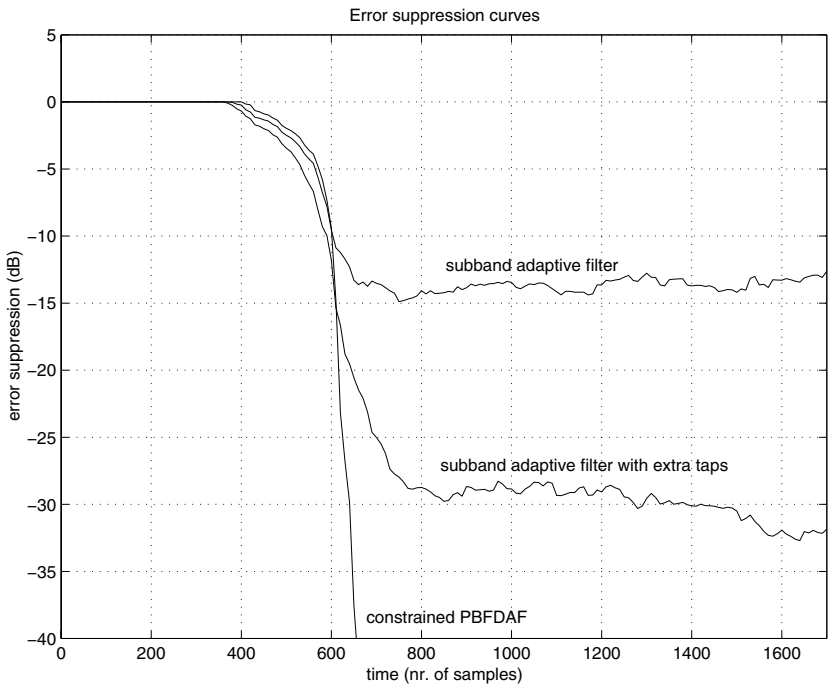


Figure 6: Convergence curves of 3 different adaptive systems. The FIR system to be identified is of order 15.

Apart from the perfect reconstruction or nearly perfect reconstruction condition, another constraint has to be imposed on the filter banks in order to cope with the undermodelling error. Consider the lower, adaptive branch in figure 1. If perfect cancellation of the far–end signal x is striven for, this branch needs to model the acoustic path $w[k]$ exactly. The lower branch can only model a time invariant system if the following condition is met (see [12]) :

$$\boldsymbol{J}\mathbf{G}^T(z)\mathrm{diag}\{F_i(z)\}\mathbf{H}(z) = \underbrace{\begin{bmatrix} W_0(z) & W_1(z) & \dots & W_{L-1}(z) \\ z^{-1}W_{L-1}(z) & W_0(z) & \dots & W_{L-2}(z) \\ \vdots & \vdots & \ddots & \vdots \end{bmatrix}}_{=\text{pseudo–circulant}} \tag{15}$$

or in case of DFT modulated filter banks :

$$\mathbf{C}(z)\mathbf{F}^{-1}\mathrm{diag}\{F_i(z)\}\mathbf{F}\mathbf{B}(z) = \underbrace{\begin{bmatrix} W_0(z) & W_1(z) & \dots & W_{L-1}(z) \\ z^{-1}W_{L-1}(z) & W_0(z) & \dots & W_{L-2}(z) \\ \vdots & \vdots & \ddots & \vdots \end{bmatrix}}_{=\text{pseudo–circulant}}. \tag{16}$$

The following time–invariant path is then being modelled :

$$\tilde{W}(z) = \sum_{l=0}^{L-1} z^{-l} W_l(z^L). \tag{17}$$

Equation 15 and 16 are necessary conditions to ensure complete modelling of the unknown system $W(z)$ with a set of adaptive filters. In general, this last condition will not be satisfied for subband adaptive systems unless the adaptive filters are infinitely long (see Eq. 14 for the case of ideal analysis/synthesis filters). In principle, a suitable filter bank set then has to be found such that any finite–order system $W(z)$ can be modelled with finite–length filters $F_i(z)$ following equation 15.

4 Frequency–Domain Adaptive Filtering

As a cheaper alternative to LMS, the frequency–domain adaptive filter (FDAF) was introduced, which is a direct translation of Block LMS in frequency domain [10], based on the well known fact that correlation (weight updating) and convolution (filtering) operations may be implemented more efficiently in frequency domain. Instead of a linear convolution/correlation a circular operation is then performed. This requires some "restore" operations which can be of the overlap–save or overlap–add type. If only the convolution operation is corrected a so–called unconstrained FDAF is obtained, requiring 3 FFTs per block update. Two more FFTs are needed for the gradient estimate correction resulting in a constrained FDAF.
A major drawback with standard frequency–domain adaptive filters is the inherent delay. Partitioning then may be used to reduce the overall delay.

4.1 Partitioned Block FDAF

By splitting the acoustic impulse response in equal parts, a kind of mixed time– and frequency–domain adaptive filter is obtained, called the Partitioned Block Frequency–Domain Adaptive Filter (PBFDAF) [3][9][11]. Here block lengths can be adjusted, resulting in a cheap adaptive filter with acceptable processing delay.
The L_{FB}–taps fullband adaptive filter $w^{(n)}[k]$ at block index n is partitioned in $\frac{L_{FB}}{P}$ equal parts $\mathbf{w}^{(n,p)}$ of length P each :[1]

$$\mathbf{w}^{(n,p)} \stackrel{\forall p}{=} \begin{bmatrix} w^{(n)}[pP] \\ \vdots \\ w^{(n)}[(p+1)P-1] \end{bmatrix}, \quad p = 0 : \frac{L_{FB}}{P} - 1 \tag{18}$$

$$\mathbf{w}_p^{(n)} \stackrel{\forall p}{=} \mathbf{F} \begin{bmatrix} \mathbf{w}^{(n,p)} \\ \mathbf{0} \end{bmatrix} \begin{matrix} \updownarrow P \\ \updownarrow L-1 \end{matrix} \tag{19}$$

[1] We assume that $\frac{L_{FB}}{P}$ is integer.

The equations defining the PBFDAF are[2] :

$$\mathbf{X}_p^{(n)} \stackrel{\forall p}{=} \text{diag}\left\{ \mathbf{F} \left[\begin{array}{c} x[(n+1)L - pP - M + 1] \\ \vdots \\ x[(n+1)L - pP] \end{array} \right] \right\} \Bigg\updownarrow M, \quad p = 0 : \frac{L_{FB}}{P} - 1 \tag{20}$$

$$\mathbf{y}^{(n)} = \left[\begin{array}{cc} \mathbf{0}_{P-1} & \mathbf{0} \\ \mathbf{0} & \mathbf{I}_L \end{array} \right] \mathbf{F}^{-1} \sum_{p=0}^{\frac{L_{FB}}{P}-1} \mathbf{X}_p^{(n)} \mathbf{w}_p^{(n)} \tag{21}$$

$$\mathbf{d}^{(n)} = \left[\begin{array}{c} \mathbf{0} \\ \mathbf{d}_n \end{array} \right] \begin{array}{l} \updownarrow P-1 \\ \updownarrow L \end{array}, \qquad \mathbf{d}_n = \left[\begin{array}{c} d[nL+1] \\ \vdots \\ d[(n+1)L] \end{array} \right] \Bigg\updownarrow L \tag{22}$$

$$\mathbf{e}^{(n)} = \mathbf{d}^{(n)} - \mathbf{y}^{(n)} \tag{23}$$

$$\mathbf{w}_p^{(n+1)} \stackrel{\forall p}{=} \mathbf{w}_p^{(n)} + \mathbf{F} \left[\begin{array}{cc} \mathbf{I}_P & \mathbf{0} \\ \mathbf{0} & \mathbf{0}_{L-1} \end{array} \right] \mathbf{F}^{-1} \mathbf{\Delta}\, \mathbf{X}_p^{(n)*}\, \mathbf{F}\mathbf{e}^{(n)} \tag{24}$$

In each iteration, L new x–samples are taken in, and L new filter output samples are produced (simular to figure 2). L is called the block length, the corresponding input/output delay is $2L-1$. $\mathbf{F}$ is an $M \times M$ DFT matrix, $\mathbf{\Delta} = 2\text{diag}(\mu_m)$ contains the subband dependent step sizes and $M = P + L - 1$. If P is divisible by L (which is typically the case), $\mathbf{X}_p^{(n)} = \mathbf{X}_0^{(n-pP/L)}$ and hence equation 20 requires only 1 DFT operation, which corresponds to $p = 0$. The other $\mathbf{X}_p^{(n)}$ can be recovered from previous iterations. In most practical applications $P = L$.
There exists two variants of this algorithm, called the constrained and the unconstrained PBFDAF. For the unconstrained version

$$\mathbf{F} \left[\begin{array}{cc} \mathbf{I}_P & \mathbf{0} \\ \mathbf{0} & \mathbf{0}_{L-1} \end{array} \right] \mathbf{F}^{-1}$$

is left out from Eq. 24. The unconstrained updating requires 3 DFTs per iteration whereas the constrained PBFDAF is more expensive, having an extra $\frac{2L_{FB}}{P}$ DFTs to compute. The latter on the other hand has better convergence properties.

4.2 M>P+L-1

In the previous paragraph M was set equal to $P + L - 1$. But if M is a power of 2 efficient FFT implementation is possible. Hence, it is often better to choose M equal to $M = P + L - 1 + s = 2^r$ with $s > 0$ and r an integer. In this case the last $L + s$ and not only the last L elements of (cf Eq. 21)

$$\mathbf{F}^{-1} \sum_{p=0}^{\frac{L_{FB}}{P}-1} \mathbf{X}_p^{(n)} \mathbf{w}_p^{(n)} \tag{25}$$

[2]For signal conventions : see figure 3

correspond to meaningful values for $\mathbf{y}^{(n)}$, not affected by circular convolution. However, an ambiguity can then occur with unconstrained PBFDAF, such that the subband filters are not uniquely defined anymore. In the unconstrained case it is not guaranteed that the $\mathbf{w}_p^{(n)}$ maintain the initial format set in equation 19. A random value ϵ can appear in equation 19 as an extra $(P+1)$–th element of $\mathbf{w}^{(n,p)}$ for instance as long as it is compensated for at the first element of $\mathbf{w}^{(n,p+1)}$. Similar terms can be added to other elements. For constrained PBFDAF the format is re–imposed in each iteration step by the weight updating formula (Eq. 24) and no ambiguity is found. It can not occur either with FDAF as $\frac{L_{FB}}{P} = 1$. As ϵ is random no control on its amplitude is possible, so there is a possibility of running into numerical trouble.
The ambiguity can be removed by taking in account $L+s$ samples instead of L to determine the error $\mathbf{e}^{(n)}$. This has an additional advantage : a more accurate gradient estimate is now computed as $L+s$ instead of L past estimates are being averaged. Block length L has remained the same, so tracking performance has not gone down.
An experiment was carried out in which a Gaussian white noise signal was fed through a random 50–th order linear FIR system w. An unconstrained PBFDAF $(M = 32, L = P = 16, L_{FB} = 64)$ was used to identify the system with and without the ambiguity compensation discussed in this paragraph. The compensation technique presented here does not seem to improve the convergence of the error signal as such, but a clear difference is noticeable if we look into the time evolution of the adaptive weights $\tilde{w}$ (**Figure 7**). Without ambiguity compensation the system is wrongly estimated.

4.3 PBFDAF as a special case of subband adaptive filtering

Figure 8 represents the partitioned block frequency–domain adaptive filter in a graphical way. Here we assume that P is divisible by L such that transformed "x–blocks" can be recuperated from previous block iterations (see section 4.1). The adaptive filters then take on the form $F_i(z^{\frac{P}{L}})$ (see also Eq. 33 and 34). It is indicated how equation 20, 21 and 22, which define the filtering part of the PBFDAF can be situated in the scheme. By comparing figure 8 with figure 1 it appears that the PBFDAF is a kind of subband adaptive system. However, instead of using the (aliased) subband errors[3] directly to update the adaptive weights, as is done in the standard subband scheme (figure 1), a "restore" operation of the type

$$\mathbf{F} \begin{bmatrix} \mathbf{I} & \mathbf{0} \\ \mathbf{0} & \mathbf{0} \end{bmatrix} \mathbf{F}^{-1}$$

projects the subband error vector to obtain the right format.
Looking closer, figure 8 can be cast in the oversampled subband framework of figure 3, i.e. with size L (instead of size M) tapped delay lines. **Figure 9** depicts

[3]These are found by subtracting the signals entering the left most IDFT block of the lower branch (see figure 8) from those entering the IDFT block in the upper branch.

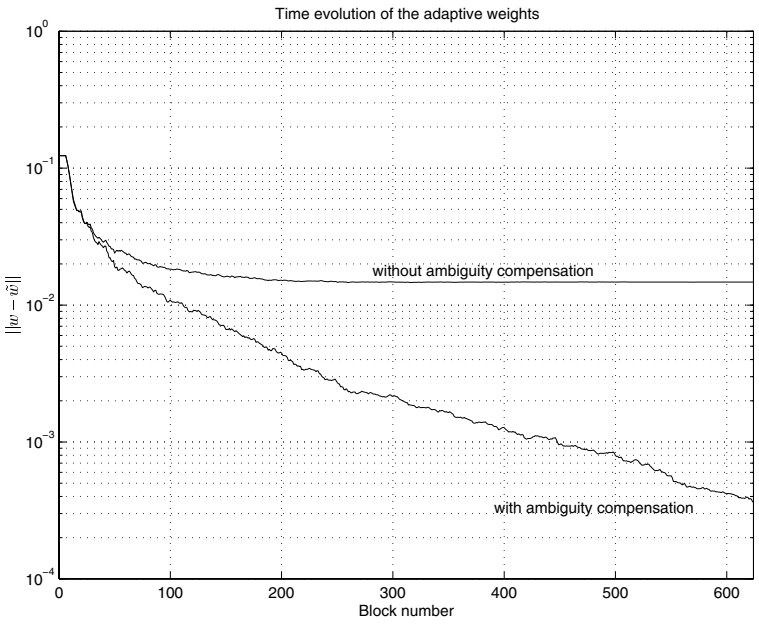


Figure 7: Ambiguity compensation : time evolution of the adaptive weights

the PBFDAF completely in the subband "jargon". An extra module called "error correction" was included which represents the "restore operation", and which is an addition to the usual subband scheme. The $\mathbf{B}(z)$–matrix for an $M-$band L–fold downsampled DFT modulated analysis filter bank is a structured matrix satisfying equation 5. The filter bank used here is a simple DFT filter bank for which

$$E_{k:K}(z) = 1 \quad \text{if } k < M \tag{26}$$
$$= 0 \quad \text{if } k \geqslant M. \tag{27}$$

Hence,

$$\underbrace{\mathbf{B}(z)}_{M\times L} = \begin{bmatrix} \mathbf{I}_L \\ z^{-1}\mathbf{I}_L \\ \vdots \\ z^{-(\lfloor\frac{M-1}{L}\rfloor-1)}\mathbf{I}_L \\ \mathbf{R}(z) \end{bmatrix} \tag{28}$$

in which $\mathbf{R}(z)$ is an $(M - L\lfloor\frac{M-1}{L}\rfloor) \times L$ matrix :

$$\mathbf{R}(z) = \begin{bmatrix} z^{-\lfloor\frac{M-1}{L}\rfloor} & \dots & 0 \\ \vdots & \ddots & \vdots \\ \dots & z^{-\lfloor\frac{M-1}{L}\rfloor} & \dots \end{bmatrix}. \tag{29}$$

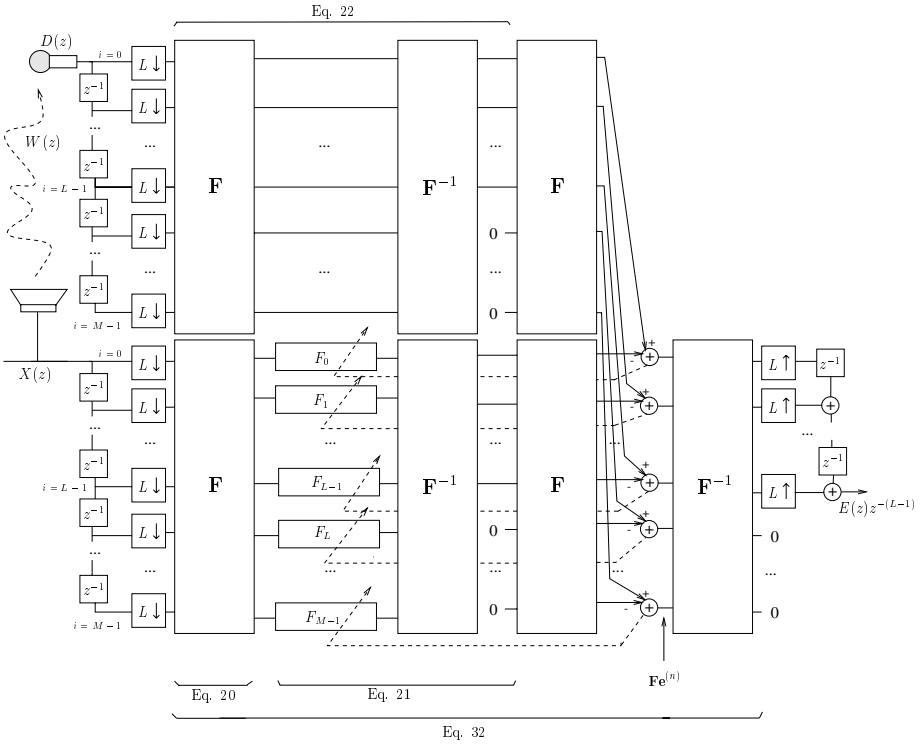


Figure 8: Partitioned block frequency–domain adaptive filtering : graphical representation

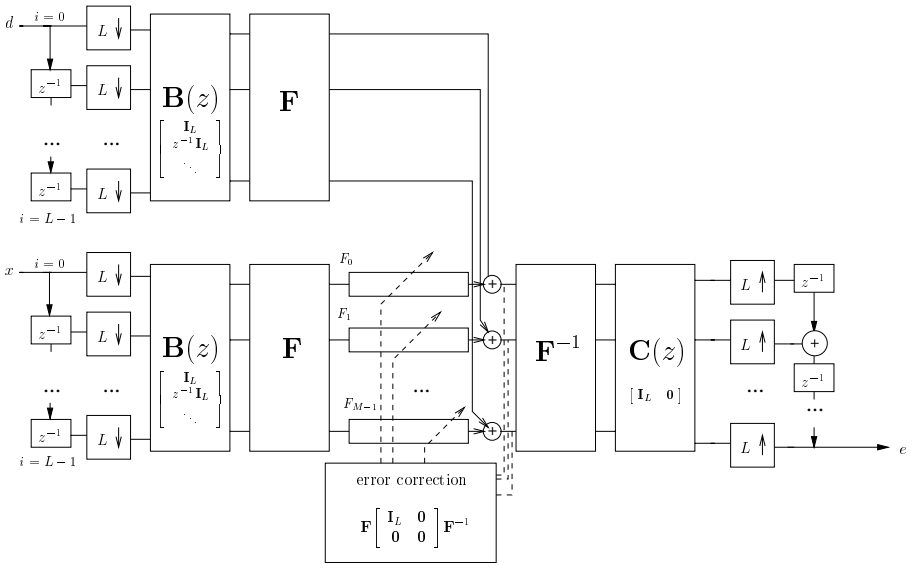


Figure 9: PBFDAF as a DFT modulated oversampled subband scheme

The frequency response of the prototype filter has a sinc–like shape with a low frequency selectivity. The analysis prototype frequency amplitude response for M=12 and L=6 is shown in **Figure 10** in full line. Also the synthesis part can be fit into the subband filter approach. The synthesis bank $\mathbf{C}(z)$–matrix is given by :

$$\underbrace{\mathbf{C}(z)}_{L\times M} = \left[\, \mathbf{I}_L \quad \mathbf{0}_L \quad \ldots \quad \mathbf{0}_L \quad \mathbf{0} \,\right] \tag{30}$$

The synthesis filters can be obtained as time–reversed and complex conjugated versions of a DFT modulated filter bank with prototype polyphase components $E_{k:K}(z) = 1$, $k < L$. The other polyphase components are zero. The synthesis prototype frequency response for M=12 and L=6 is shown in figure 10 in dashed dotted line. Its frequency response is twice as wide as the analysis prototype. A filter bank with sinc–shaped frequency amplitude response only shows a poor frequency selectivity. Inter–subband aliasing can not be avoided in this case. However, the overlap–save procedure assures appropriate convergence of the adaptive filters. This is illustrated by means of the following simulation example.

4.4 Simulation example

In **Figure 11** three frequency–domain/subband algorithms are compared. A random FIR system of order 15 was generated and fed with white noise. The constrained PBFDAF, the unconstrained PBFDAF and a true subband adaptive filter are compared. All adaptation schemes are unnormalised. The true

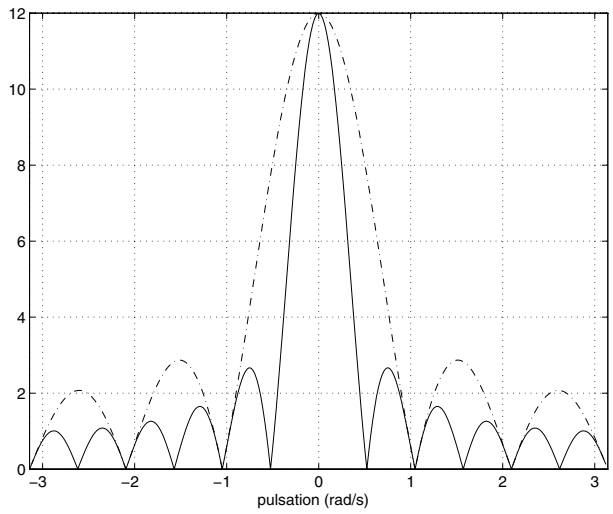


Figure 10: Analysis and synthesis bank prototype filters for the PBFDAF

subband algorithm uses the same filter banks as the (un)constrained PBFDAF but the overlap–save compensation on the error signal (cf. error correction in figure 9) is left out. In this way the subband filters are adapted on the subband errors directly. All algorithms can be considered as subband adaptive systems. They all have 8 subbands which are 4–fold subsampled and the subband filters have 4 taps each. No anti–causal taps were added. The constrained PBFDAF clearly outperforms the unconstrained PBFDAF, whereas for the subband algorithm without error compensation a considerable undermodelling error remains. It is remarkable how an unselective filter bank can lead to satisfactory results if appropriate compensation is provided.

4.5 PBFDAF : realisation conditions

By filling in Eq. 28 and 30 in Eq. 7 it is easily verified that the perfect reconstruction condition is fulfilled for the PBFDAF :

$$\left[\begin{array}{cccc} \mathbf{I}_L & \mathbf{0}_L & \dots & \mathbf{0} \end{array} \right] \left[\begin{array}{c} \mathbf{I}_L \\ z^{-1}\mathbf{I}_L \\ \vdots \\ \mathbf{R}(z) \end{array} \right] = \mathbf{I}_L. \tag{31}$$

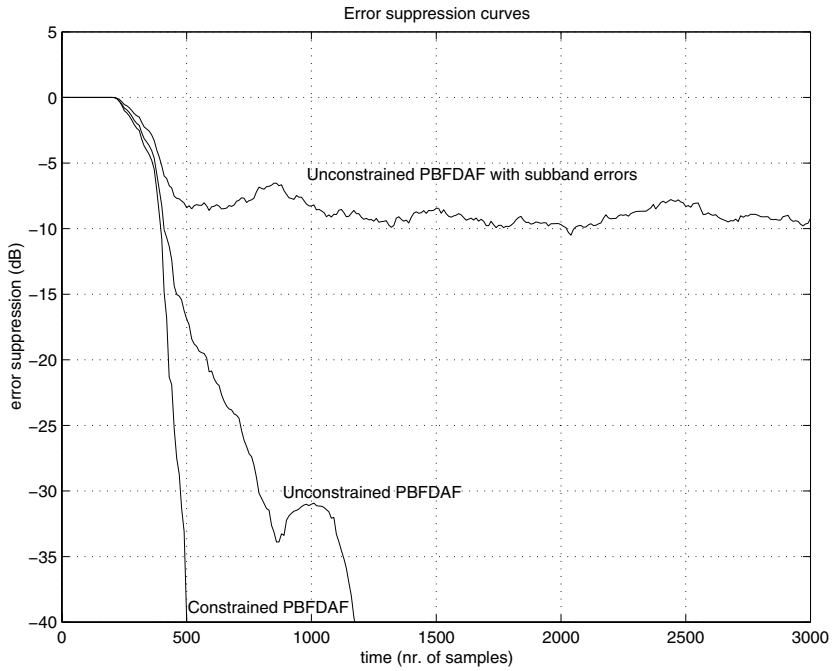


Figure 11: Convergence curves of 3 frequency–domain algorithms

For the time–invariance condition (Eq. 16) to be satisfied,

$$\left[\begin{array}{cccc} \mathbf{I}_L & \mathbf{0}_L & \dots & \mathbf{0} \end{array}\right] \mathbf{F}^{-1} \mathrm{diag}\{F_i(z)\} \mathbf{F} \left[\begin{array}{c} \mathbf{I}_L \\ z^{-1}\mathbf{I}_L \\ \vdots \\ \mathbf{R}(z) \end{array}\right] \tag{32}$$

has to be a pseudo–circulant $L \times L$ matrix. As indicated on figure 8, equation 32 is equivalent to the lower branch of the adaptive scheme.
It is well–known that a circulant matrix can be diagonalised using DFT–operations. Hence, a set of subband filters $F_i(z)$ can be found such that

$$\mathbf{F}^{-1} \mathrm{diag}\{F_i(z)\} \mathbf{F} = \mathbf{M}(z^{1/L}), \tag{33}$$

with $\mathbf{M}(z)$ the following circulant $M \times M$ matrix :

$$\mathbf{M}(z) = \begin{bmatrix} W_0(z^P) & \dots & W_{P-1}(z^P) & 0 & \dots & 0 \\ 0 & W_0(z^P) & \dots & W_{P-1}(z^P) & \dots & 0 \\ \vdots & \ddots & \ddots & \ddots & \ddots & \vdots \\ 0 & \dots & 0 & W_0(z^P) & \dots & W_{P-1}(z^P) \\ W_{P-1}(z^P) & \dots & 0 & 0 & W_0(z^P) & \dots \\ \vdots & \ddots & \ddots & \ddots & \ddots & \vdots \\ W_1(z^P) & \dots & 0 & 0 & \dots & W_0(z^P) \end{bmatrix} . \tag{34}$$

The $F_i(z)$ will correspond to the DFT coefficients of the first column of $\mathbf{M}(z^{1/L})$, where $W(z) = \sum_{p=0}^{P-1} z^{-p} W_p(z^P)$ is the channel to be modelled (figure 1). Now, element (i,j) of $L \times L$ matrix $\mathbf{C}(z)\mathbf{F}^{-1}\text{diag}\{F_i(z)\}\mathbf{FB}(z)$ can be written as

$$\sum_{n=-\infty}^{\infty} z^{-n} W_{j-i+nL}(z^{\frac{P}{L}}) \qquad \text{with } W_p = 0 \quad \text{if } p < 0 \text{ or } p \geqslant P \tag{35}$$

An $L \times L$ matrix $\mathbf{T}(z)$ is pseudo–circulant if

1. all elements $T_{m,n}(z)$ of $\mathbf{T}(z)$ on the same diagonal are equal
2. $T_{i,L-1}(z) = zT_{i+1,0}(z)$, for all i

Expression 35 depends on $j-i$ and hence all elements on the same diagonal are equal. Furthermore, element $(i, L-1)$ is

$$\sum_{n=-\infty}^{\infty} z^{-n} W_{L-1-i+nL}(z^{\frac{P}{L}}) \overset{m=n+1}{=} z \sum_{m=-\infty}^{\infty} z^{-m} W_{-i-1+mL}(z^{\frac{P}{L}}) \tag{36}$$

which is element $(i+1, 0)$ multiplied by z and hence equation 32 is indeed pseudo–circulant. From equation 16, 17 and 35 we know that equation 32 models the following time–invariant system :

$$\tilde{W}(z) = \sum_{l=0}^{L-1} \sum_{n=-\infty}^{\infty} z^{-nL-l} W_{l+nL}(z^P) \tag{37}$$

$$= \sum_{p=0}^{P-1} z^{-p} W_p(z^P) \tag{38}$$

and hence W_p are the P–th order polyphase components of $\tilde{W}(z)$. If the W_p are of finite length and P is a multiple of L, also the F_i will be of finite length (Eq. 33), and hence exact modelling of a finite–order system $\tilde{W}(z)$ using finite–length filters $F_i(z)$ is feasible. It appears that for the PBFDAF the above mentioned conditions of perfect reconstruction and perfect path modelling are indeed fulfilled. The first realisation condition requiring frequency selective filter banks is only met to a certain extent (see paragraph 4.3).

5 Alternative Adaptation Scheme

From experimental results (see e.g. figure 6) it appears that frequency–domain adaptive filters such as the PBFDAF outperform standard subband systems despite their low implementation cost. It is therefore believed that a class of subband adaptive systems can be defined which adopt mechanisms and properties of the frequency–domain approach (e.g. realisation conditions) such that they approximate the performance of the PBFDAF.
In an attempt to generalise the frequency–domain error correction to subband adaptive systems, we now focus on an alternative adaptation scheme for subband adaptive systems which adjusts the subband filters F_m (see **Figure 12**) based on the fullband error e instead of using the subband error signals $\epsilon_m = d_m - y_m$ as is normally done in a standard subband scheme (see figure 1).

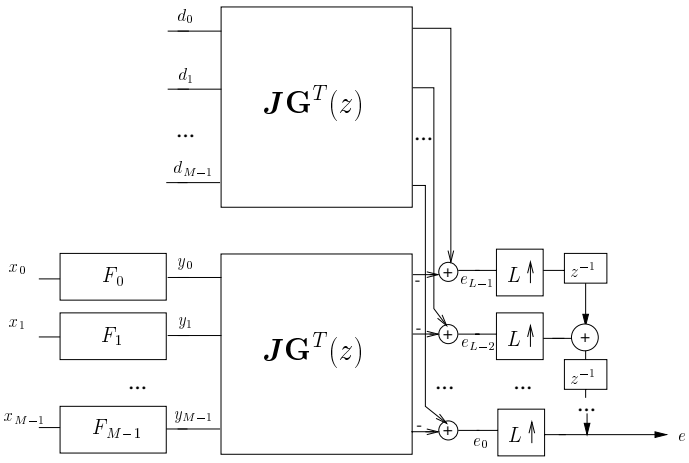


Figure 12: Oversampled subband adaptive filter : synthesis part

5.1 Fullband error adaptation scheme

Define :

$$\underbrace{\begin{bmatrix} \mathbf{y}_0^k \\ \vdots \\ \mathbf{y}_{M-1}^k \end{bmatrix}}_{\mathbf{y}_k} = \underbrace{\begin{bmatrix} \mathbf{X}_0^k & \dots & \mathbf{0} \\ \vdots & \ddots & \vdots \\ \mathbf{0} & \dots & \mathbf{X}_{M-1}^k \end{bmatrix}}_{\mathbf{X}_k} \underbrace{\begin{bmatrix} \mathbf{f}_0^k \\ \vdots \\ \mathbf{f}_{M-1}^k \end{bmatrix}}_{\mathbf{w}_k}, \tag{39}$$

in which (see figure 12)

$$\mathbf{X}_m^k = \underbrace{\begin{bmatrix} x_m[k-L_f+1] & \dots & x_m[k-L_f-L_{SB}+2] \\ \vdots & \ddots & \vdots \\ x_m[k] & \dots & x_m[k-L_{SB}+1] \end{bmatrix}}_{L_{SB}} \Big\updownarrow L_f, \tag{40}$$

$$\mathbf{f}_m^k = \begin{bmatrix} f_m^k[0] \\ \vdots \\ f_m^k[L_{SB}-1] \end{bmatrix} \Big\updownarrow L_{SB}, \quad \mathbf{y}_m^k = \begin{bmatrix} y_m[k-L_f+1] \\ \vdots \\ y_m[k] \end{bmatrix} \Big\updownarrow L_f \tag{41}$$

$\mathbf{w}_k$ is the adaptive filter vector. L_{SB} is the length[4] of the subband adaptive filters, L_f is the length of the synthesis bank polyphase filters. Further define

$$\underbrace{\begin{bmatrix} e_0[k] \\ \vdots \\ e_{L-1}[k] \end{bmatrix}}_{\mathbf{e}_k^{FB}} = \underbrace{\begin{bmatrix} \mathbf{s}_{0_{0:L}} & \dots & \mathbf{s}_{M-1_{0:L}} \\ \vdots & \ddots & \vdots \\ \mathbf{s}_{0_{L-1:L}} & \dots & \mathbf{s}_{M-1_{L-1:L}} \end{bmatrix}}_{\mathbf{S}^T} \underbrace{\begin{bmatrix} \boldsymbol{\epsilon}_0^k \\ \vdots \\ \boldsymbol{\epsilon}_{M-1}^k \end{bmatrix}}_{\mathbf{e}_k^{SB}} \tag{42}$$

in which

$$\underbrace{\begin{bmatrix} \boldsymbol{\epsilon}_0^k \\ \vdots \\ \boldsymbol{\epsilon}_{M-1}^k \end{bmatrix}}_{\mathbf{e}_k^{SB}} = \underbrace{\begin{bmatrix} \mathbf{d}_0^k \\ \vdots \\ \mathbf{d}_{M-1}^k \end{bmatrix}}_{\mathbf{d}_k} - \underbrace{\begin{bmatrix} \mathbf{y}_0^k \\ \vdots \\ \mathbf{y}_{M-1}^k \end{bmatrix}}_{\mathbf{y}_k}, \tag{43}$$

$$\mathbf{d}_m^k = \begin{bmatrix} d_m[k-L_f+1] \\ \vdots \\ d_m[k] \end{bmatrix} \Big\updownarrow L_f, \quad \boldsymbol{\epsilon}_m^k = \begin{bmatrix} \epsilon_m[k-L_f+1] \\ \vdots \\ \epsilon_m[k] \end{bmatrix} \Big\updownarrow L_f, \tag{44}$$

$$\mathbf{s}_{m_{l:L}} = \underbrace{\begin{bmatrix} g_{m_{l:L}}[L_f-1] & \dots & g_{m_{l:L}}[0] \end{bmatrix}}_{L_f}. \tag{45}$$

$\mathbf{e}_k^{FB}$ is the fullband error vector, $\mathbf{e}_k^{SB}$ contains the subband errors, $\mathbf{S}$ represents the synthesis filter bank and $g_{m_{l:L}}[k] = g_m[kL+l]$ is the l–th out of L polyphase components of the m–th synthesis filter $g_m[k]$.
Optimal error suppression is obtained when Eq. 42 is as small as possible :

$$\min_{\mathbf{w}_k} \mathcal{E}\left\{||\mathbf{e}_k^{FB}||_2^2\right\} \tag{46}$$

The optimal $\mathbf{w}$ is

$$\mathbf{w}_{\text{opt}} = \arg\min_{\mathbf{w}_k} ||\mathbf{S}^T\mathbf{d}_k - \mathbf{S}^T\mathbf{X}_k\mathbf{w}_k||_2^2. \tag{47}$$

[4]We assume that all filters are FIR.

In practice the optimal subband filters are estimated adaptively using a steepest descent algorithm. The gradient with respect to $\mathbf{w}_k$ is

$$\nabla \mathbf{w}_k = 2\mathbf{X}_k^H \mathbf{S}^* \mathbf{S}^T (\mathbf{X}_k \mathbf{w}_k - \mathbf{d}_k). \tag{48}$$

Therefore, $\mathbf{w}_{\text{opt}}$ can be found in an iterative way using a fullband error block adaptation algorithm :

$$\begin{aligned} \mathbf{w}_{k+1} &= \mathbf{w}_k + 2\mathbf{\Delta} \mathbf{X}_k^H \mathbf{S}^* \mathbf{S}^T (\mathbf{d}_k - \mathbf{X}_k \mathbf{w}_k) & (49) \\ &= \mathbf{w}_k + 2\mathbf{\Delta} \mathbf{X}_k^H \mathbf{S}^* \mathbf{S}^T \mathbf{e}_k^{SB} & (50) \end{aligned}$$

with $\mathbf{\Delta} = \text{diag}(\mu_m)$ a diagonal matrix with subband dependent stepsizes. The subband errors are passed through the synthesis bank twice before they are combined with the far–end signal x.
In a standard subband adaptation scheme the subband errors are minimised, leading to

$$\min_{\mathbf{w}_k} \mathcal{E} \left\{ ||\mathbf{e}_k^{SB}||_2^2 \right\}. \tag{51}$$

The gradient with respect to $\mathbf{w}_k$ is

$$\nabla \mathbf{w}_k = 2\mathbf{X}_k^H (\mathbf{X}_k \mathbf{w}_k - \mathbf{d}_k). \tag{52}$$

Therefore, the optimal $\mathbf{w}$ can be found in an iterative way using subband errors:

$$\mathbf{w}_{k+1} = \mathbf{w}_k + 2\mathbf{\Delta} \mathbf{X}_k^H \mathbf{e}_k^{SB}. \tag{53}$$

In practice,

$$\mathbf{w}_{k+1} = \mathbf{w}_k + 2\mathbf{\Delta} \mathbf{X}_k^H \begin{bmatrix} \boldsymbol{\mathcal{D}} & \dots & \mathbf{0} \\ \vdots & \ddots & \vdots \\ \mathbf{0} & \dots & \boldsymbol{\mathcal{D}} \end{bmatrix} \mathbf{e}_k^{SB} \tag{54}$$

is often used with $\boldsymbol{\mathcal{D}}$ an $L_f \times L_f$ diagonal matrix with only 1 element different from 0 :

$$\boldsymbol{\mathcal{D}} = \left[\begin{array}{c|c} \mathbf{0}_{(L_f-1)\times(L_f-1)} & \mathbf{0} \\ \hline \mathbf{0} & 1 \end{array} \right] \tag{55}$$

Equation 54 corresponds to a standard subband weight updating algorithm using the LMS algorithm in each subband. Equation 53 corresponds to a standard subband weight updating algorithm using a block–LMS algorithm in each band. Remark that the compensation matrix $\mathbf{S}^* \mathbf{S}^T$ is absent in Eq. 53 and 54. It is hoped that employing the fullband error adaptation scheme will lead to improved performance.

5.2 Computational complexity

To update the weights with the fullband error adaptation scheme, the subband errors are passed through the synthesis bank twice (Eq. 50). The corresponding

cost is therefore rather high. As $\mathbf{S}$ is an $ML_f \times L$ matrix, the extra cost compared to a subband–error based adaptation will be[5]

$$\begin{array}{ll} LML_f \text{ cplx MACs} & \text{for } \mathbf{S}^T * \text{vector} \\ LML_f \text{ cplx MACs} & \text{for } \mathbf{S}^* * \text{vector} \end{array}$$

Only when $L_f = 1$ it might be better to compute $\mathbf{S}^*\mathbf{S}^T$ beforehand and calculate $(\mathbf{S}^*\mathbf{S}^T)\mathbf{e}_k^{SB}$ directly. The cost would be

$$M^2 L_f^2 \text{ cplx MACs}$$

in that case.
The cost reduces however when the filter banks are DFT modulated and e is a real signal. Only half of the subbands need to be computed as they are pairwisely complex conjugated. Furthermore, $\mathbf{S}^*\mathbf{S}^T$ can be simplified. For DFT modulated filter banks the transpose of the synthesis bank polyphase matrix can be written as

$$\mathbf{G}^T(z) = \boldsymbol{J}\mathbf{C}(z)\mathbf{F}^{-1}. \tag{56}$$

$\mathbf{S}^T$ as defined in Eq. 42 and 45 is closely related to $\mathbf{G}^T(z)$ and can be expressed as

$$\mathbf{S}^T = \boldsymbol{J}\mathbf{Q}\hat{\mathbf{F}}^{-1}. \tag{57}$$

$\hat{\mathbf{F}}$ is an extended DFT matrix and can be defined as the Kronecker product of a DFT matrix and an identity matrix

$$\hat{\mathbf{F}} = \mathbf{F} \otimes \mathbf{I}_{L_f}. \tag{58}$$

$\mathbf{Q}$ is a block $L \times M$ matrix and is constructed from $\mathbf{C}(z)$ in the same way as $\mathbf{S}^T$ was derived from $\mathbf{G}^T(z)$. Hence, each block element of $\mathbf{Q}$ is a real–valued $1 \times L_f$ vector such that $\mathbf{Q}$ becomes

$$\begin{bmatrix} c_{0,0}[L_f-1] & \dots & c_{0,0}[0] & \dots & c_{0,M-1}[L_f-1] & \dots & c_{0,M-1}[0] \\ \vdots & & & \ddots & & & \vdots \\ c_{L-1,0}[L_f-1] & \dots & c_{L-1,0}[0] & \dots & c_{L-1,M-1}[L_f-1] & \dots & c_{L-1,M-1}[0] \end{bmatrix}. \tag{59}$$

$c_{n,m}$ refers to element (n,m) of $\mathbf{C}(z)$, which is equal to $c_{n,m}[0] + z^{-1}c_{n,m}[1] + \cdots + z^{-L_f+1}c_{n,m}[L_f-1]$. Equation 50 becomes

$$\mathbf{w}_{k+1} = \mathbf{w}_k + \frac{2}{M}\boldsymbol{\Delta}\mathbf{X}_k^H\hat{\mathbf{F}}\mathbf{Q}^T\mathbf{Q}\hat{\mathbf{F}}^{-1}\mathbf{e}_k^{SB}. \tag{60}$$

The matrix–vector product $\hat{\mathbf{F}}^{-1}\mathbf{e}_k^{SB}$ comes down to a set of IFFT–operations : for each of the L_f time–lags in $\mathbf{e}_k^{SB}$ an M–point IFFT needs to be computed. The algorithm can be further simplified as $L_f - 1$ IFFTs can be taken from previous

[5] *cplx MAC* stands for a complex multiply–accumulate operation and comes down to a complex multiplication and a complex addition, which is equivalent to 4 real multiplications and 4 real additions.

blocks. Although this simplification is only approximate, the performance stays more or less the same.
For DFT modulated filter banks $\mathbf{C}(z)$ typically has the same structure as $\mathbf{B}(z)$ and hence it is a sparse matrix (see Eq. 5). As a result only about LL_f of the LML_f elements of $\mathbf{Q}$ are non–zero. The cost associated with $\frac{1}{M}\hat{\mathbf{F}}\mathbf{Q}^T\mathbf{Q}\hat{\mathbf{F}}^{-1}$ therefore is

$2M\log_2 M$ ops	for an M–point real–output IFFT
LL_f real MACs	for $\mathbf{Q}*$vector
LL_f real MACS	for $\mathbf{Q}^T*$vector
$L_f(2M\log_2 M - 4M + 6)$ ops	for L_f M–point real–input FFTs

5.3 PBFDAF weight updating

The alternative adaptation scheme studied in paragraph 5.1, leading to a weight updating equation based on fullband errors (Eq. 50) is reconsidered and applied to the PBFDAF. For DFT modulated filter banks the synthesis bank polyphase matrix $\mathbf{G}(z)$ can be written as

$$\mathbf{F}^{-T}\mathbf{C}^T(z)\boldsymbol{J}. \tag{61}$$

For PBFDAF for which P a multiple of L

$$\mathbf{C}(z) = \underbrace{\left[\begin{array}{cccc}\mathbf{I}_L & \mathbf{0}_L & \ldots & \mathbf{0}_L \quad \mathbf{0}\end{array}\right]}_{M} = \mathbf{C} = \mathbf{Q} \tag{62}$$

is independent of z and hence also $\mathbf{G}(z)$ is independent of z. This means the synthesis polyphase filters have length $L_f = 1$. $\mathbf{S}$ as defined in Eq. 42 then equals $\mathbf{G}(z) = \mathbf{S} = \mathbf{F}^{-T}\mathbf{C}^T\boldsymbol{J}$. For the PBFDAF the update equation 50 becomes

$$\begin{aligned}\mathbf{w}_{k+1} &= \mathbf{w}_k + 2\frac{\boldsymbol{\Delta}}{M}\mathbf{X}_k^H\mathbf{F}\mathbf{C}^T\mathbf{C}\mathbf{F}^{-1}(\mathbf{d}_k - \mathbf{X}_k\mathbf{w}_k) &(63)\\ &= \mathbf{w}_k + 2\frac{\boldsymbol{\Delta}}{M}\mathbf{X}_k^H\mathbf{F}\left[\begin{array}{cc}\mathbf{I}_L & \mathbf{0}\\ \mathbf{0} & \mathbf{0}_{M-L}\end{array}\right]\mathbf{F}^{-1}\mathbf{e}_k^{SB} &(64)\end{aligned}$$

$\mathbf{e}_k^{SB}$ are the subband errors, $\mathbf{F}\mathbf{C}^T\mathbf{C}\mathbf{F}^{-1}$ does the error correction. It can be proven [6] that the weight update equation of a so–called unconstrained PBFDAF[6] [4][9]

$$\mathbf{w}_p^{(n+1)} \stackrel{\forall p}{=} \mathbf{w}_p^{(n)} + \boldsymbol{\Delta}\ \mathbf{X}_p^{(n)*}\ \mathbf{F}\mathbf{e}^{(n)} \tag{65}$$

is closely related to equation 64, derived here based on fullband error feedback. One can observe that the subband filters are adapted based on corrected subband errors. The correction implies passing the subband errors through the synthesis filter bank in order to obtain a fullband, i.e. an aliasing–free, error signal. This in fact refers to the overlap–save or overlap–add procedure upon which frequency–domain techniques are based and also corresponds to the error

[6] with P a multiple of L

correction module which was added in figure 9. It is believed that a more general class of subband adaptive systems which are based on a filter bank set fulfilling the 3 realisation conditions of frequency selectivity, perfect reconstruction and perfect path modelling, and provided with the adaptation mechanism presented in paragraph 5.1, will approximate the performance of the frequency–domain approach.

5.4 Simulation example

Again a random FIR system of order 15 was generated and fed with white noise. A 6–band, 4–fold downsampled analysis/synthesis filter bank set was designed, fulfilling the perfect reconstruction property (Eq. 7). Both the analysis and the synthesis filters are FIR, DFT modulated and are of order 27. The frequency characteristic of the analysis prototype filter are shown in **figure 13**. Based

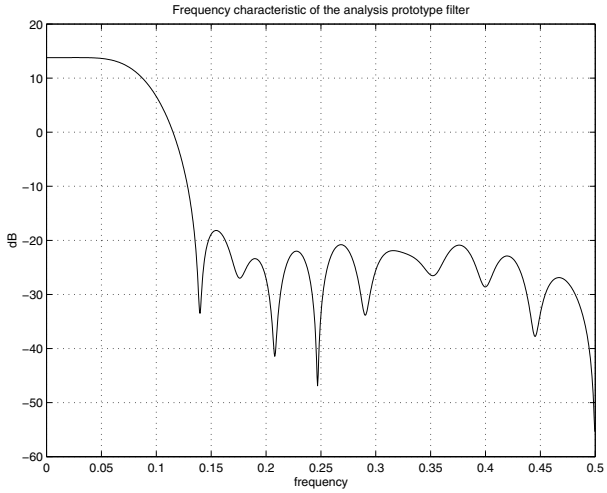


Figure 13: Simulation example : frequency characteristic of the analysis prototype filter

on this filter bank set, different subband adaptive filters are compared. They all have subband filters of length $\frac{L_{FB}}{L} = 4$, no extra taps were added. The time evolution of the error for the following subband adaptive filters is shown on **Figure 14** : a standard subband adaptive system (see figure 1 and Eq. 54) with LMS–adapted subband filters (upper curve), a subband adaptive filter using block–LMS weight updating according to Eq. 53 (middle curve) and a subband implementation using the fullband error adaptation scheme presented in Eq. 50 (bottom curve). The fullband error scheme clearly outperforms the standard subband adaptive filter.

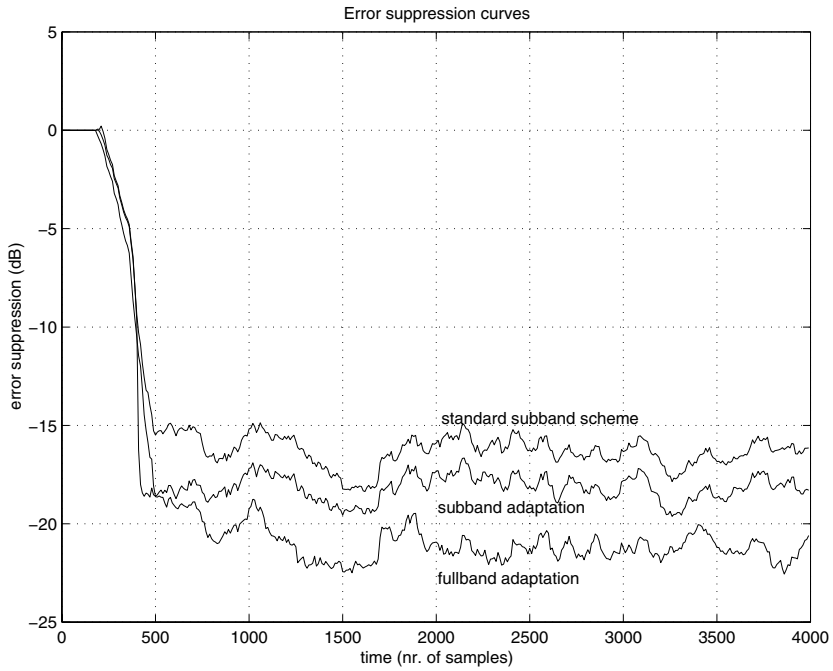


Figure 14: Simulation example : convergence curves of 3 different adaptive systems. The FIR system to be identified is of order 15.

6 Conclusions

The identification of high–order FIR systems requires efficient adaptive algorithms. Both the subband and frequency–domain approach turn out to have their strong and weak points. We specified 3 conditions for appropriate subband modelling and presented an adaptation scheme that feeds back the fullband error. The PBFDAF turns out to be a special case of subband adaptive filtering satisfying 2 realisation conditions and offering a satisfactory performance at a low implementation cost, despite the low frequency–selective filter banks it is based on. The fullband error adaptation scheme can be considered as a generalisation and extension of the frequency–domain error correction technique and is believed to provide a useful additional module to improve performance in subband adaptive systems.

7 Acknowledgements

The authors would like to thank Ian Proudler for his contribution to the presented work. Marc Moonen is a Research Associate with the F.W.O. (Fund for Scientific Research – Flanders). This research work was carried out at

the ESAT laboratory of the Katholieke Universiteit Leuven, in the frame of the Belgian State Interuniversity Poles of Attraction Programme – IUAP P4–02 (1997–2001) : Modeling, Identification, Simulation and Control of Complex Systems, Concerted Research Action MIPS ('Model–based Information Processing Systems') and GOA–MEFISTO–666 of the Flemish Government, Research Project F.W.O. nr. G.0295.97 ('Design and implementation of adaptive digital signal processing algorithms for broadband applications') and IWT project AUT/970517: MUSETTE ('Multimicrophone Signal Enhancement Techniques for handsfree telephony and voice controlled systems'). The scientific responsibility is assumed by its authors.

References

[1] B. Farhang–Boroujeny, *Adaptive Filters – Theory and Applications*, Wiley & Sons Ltd, West Sussex, England, 1998.

[2] Z. Cvetković, "Oversampled modulated filter banks and tight gabor frames in $l^2(\mathbb{Z})$," *Proceedings of the 1995 IEEE Int. Conf. on Acoust., Speech and Signal Processing*, Detroit, MI, May 1995, pp. 1456–1459.

[3] G. Egelmeers, P. Sommen and J. de Boer, "Realization of an acoustic echo canceller on a single DSP," *Proceedings of the European Signal Processing Conference (EUSIPCO–96)*, Trieste, Italy, September 1996, pp. 33–36.

[4] K. Eneman and M. Moonen, "Filter bank constraints for subband and frequency–domain adaptive filters," *Proceedings of the 1997 IEEE Workshop on Applications of Signal Processing to Audio and Acoustics*, New Paltz, NY, October 1997, pp. 19–22.

[5] K. Eneman and M. Moonen, "DFT Modulated Filter Bank Design for Oversampled Subband Systems," *Proceedings of the IEEE Benelux Signal Processing Symposium*, Leuven, Belgium, March 1998, pp. 87–90.

[6] K. Eneman and M. Moonen, "A fullband error adaptation scheme for subband adaptive filters," Tech. Rep. 99–103 (ftp.esat.kuleuven.ac.be/pub/sista/eneman/reports/99-103.ps.gz), ESAT–SISTA, Katholieke Universiteit Leuven, Belgium, December 1999.

[7] K. Eneman and M. Moonen, "On the length of subband adaptive filters," Tech. Rep. 00–02 (ftp.esat.kuleuven.ac.be/pub/sista/eneman/reports/00-2.ps.gz), ESAT–SISTA, Katholieke Universiteit Leuven, Belgium, January 2000.

[8] A. Gilloire and M. Vetterli, "Adaptive filtering in subbands with critical sampling : analysis, experiments and application to acoustic echo cancellation," *IEEE Trans. Signal Processing*, vol. 40, August 1992, pp. 1862–1875.

[9] J. Páez Borrallo and M. García Otero, "On the implementation of a partitioned block frequency domain adaptive filter (PBFDAF) for long acoustic echo cancellation," *Signal Processing*, vol. 27, June 1992, pp. 301–315.

[10] J. Shynk, "Frequency–domain and multirate adaptive filtering," *IEEE Signal Processing Magazine*, January 1992, pp. 15–37.

[11] J.–S. Soo and K. Pang, "Multidelay block frequency domain adaptive filter," *IEEE Trans. Acoust., Speech and Signal Processing*, vol. 38, February 1990, pp. 373–376.

[12] P. Vaidyanathan, *Multirate Systems and Filter Banks*, Prentice Hall, Englewood Cliffs, NJ, 1993.